

AperTO - Archivio Istituzionale Open Access dell'Università di Torino

A syndromic extreme insulin resistance caused by biallelic POC1A mutations in exon 10

This is the author's manuscript

Original Citation:

Availability:

This version is available <http://hdl.handle.net/2318/1650338> since 2017-10-25T16:51:30Z

Published version:

DOI:10.1530/EJE-17-0431

Terms of use:

Open Access

Anyone can freely access the full text of works made available as "Open Access". Works made available under a Creative Commons license can be used according to the terms and conditions of said license. Use of all other works requires consent of the right holder (author or publisher) if not exempted from copyright protection by the applicable law.

(Article begins on next page)



UNIVERSITÀ DEGLI STUDI DI TORINO

This is an author version of the contribution published on:

Questa è la versione dell'autore dell'opera:

[Eur J Endocrinol. 2017 Nov;177(5):K21-K27. doi: 10.1530/EJE-17-0431.]

The definitive version is available at:

La versione definitiva è disponibile alla URL:

[<http://www.eje-online.org/content/177/5/K21.long>]

**A SYNDROMIC EXTREME INSULIN RESISTANCE CAUSED BY BIALLELIC *POCIA*
MUTATIONS IN EXON 10**

Elisa Giorgio ^{1*}, Elisa Rubino ^{2,3*}, Alessandro Bruselles ⁴, Simone Pizzi ⁵, Innocenzo Rainero ²,
Sergio Duca³, Fabio Sirchia ^{1,6}, Barbara Pasini ^{1,6}, Marco Tartaglia ⁵, Alfredo Brusco ^{1,6}

¹ Department of Medical Sciences, University of Torino, 10126, Torino, Italy

² Department of Neuroscience “Rita Levi Montalcini”, University of Torino, 10126, Torino, Italy

³ Koelliker Hospital, 10134, Torino, Italy

⁴ Department of Oncology and Molecular Medicine, Istituto Superiore di Sanità, 00161, Rome, Italy.

⁵ Genetics and Rare Diseases Research Division, Ospedale Pediatrico Bambino Gesù IRCSS, 00146, Rome, Italy.

⁶ Medical Genetics Unit, Città della Salute e della Scienza University Hospital, 10126, Torino, Italy

Corresponding author: Alfredo Brusco, University of Torino, Department of Medical Sciences, via Santena 19, 10126, Torino, Italy. Fax +390116706582; e-mail: alfredo.brusco@unito.it

Short title: Clinical heterogeneity of *POCIA* mutations.

Keywords: *POCIA*; insulin resistance; short stature; SOFT syndrome, diabetes.

Word count: 2278

ABSTRACT (max 250 words)

POCIA encodes a protein with a role in centriole assembly and stability, and in ciliogenesis.

Biallelic loss of function mutations affecting *POCIA* cause SOFT syndrome, an ultra-rare condition characterized by short stature, onychodysplasia, facial dysmorphism and hypotrichosis.

Using exome sequencing, we identified a homozygous frameshift mutation (c.1047_1048dupC; p.G337Rfs*25) in a patient presenting with short stature, facial hirsutism, alopecia, dyslipidemia and extreme insulin resistance. The truncating variant affected exon 10, which is retained in only two of the three *POCIA* mature RNAs, due to alternative processing of the transcript.

Clinical discrepancies with SOFT syndrome support the hypothesis that *POCIA* mutations affecting exon 10 are associated with a distinct condition, corroborating a previous hypothesis based on a similar case. Furthermore, this report provides an additional example of a genetic condition presenting with clinical heterogeneity due to alternative transcript processing. In conclusion, mutations in *POCIA* exons 10 should be taken into account in patients with extreme insulin resistance and short stature.

1. INTRODUCTION

Proteome Of Centriole 1A (POC1A) plays a central role in early phases of centriole duplication, as well as in the later steps of centriole length control, ensuring centriole integrity and proper mitotic spindle formation ¹. Together with POC1B, it is an essential protein for ciliogenesis. Homozygous or compound heterozygous mutations in *POCIA* (#MIM 614783) cause Short stature, Onychodysplasia, Facial dysmorphism, and hypoTrichosis (SOFT) syndrome (#MIM 614813). At present, nine families with SOFT syndrome carrying a total of seven different biallelic *POCIA* mutations have been described ²⁻⁶. Major clinical features of SOFT syndrome include severe growth retardation, which occurs prenatally, facial dysmorphism (dolichocephaly, triangular elongated face, prominent forehead, ear abnormalities, prominent nose and pointy chin), brachydactyly and other skeletal features (osteopenia, short carpals, metacarpals, tarsals and metatarsals tubular bones), hypoplastic finger nails, and postpuberal hypotrichosis. Clinical findings in a subset of SOFT patients also include relative macrocephaly, type 2 diabetes, developmental delay, and hypogonadism in males.

Patients' cells show an abnormal mitotic mechanism with multipolar spindles and clearly impaired ciliogenesis ⁶.

Recently, a homozygous frameshift mutation in exon 10 of the *POCIA* gene has been reported in a woman of Italian origin with clinical features of primordial dwarfism, skeletal dysplasia, facial dysmorphism, extreme dyslipidemia with insulin resistance and fatty liver, which only in part were reminiscent of SOFT syndrome ⁷. The authors suggested that, differently from what observed for the mutations causing SOFT syndrome, the mutation in exon 10 affects only two of the three POC1A isoforms generated by alternative processing of the *POCIA* transcript, preserving the isoform lacking exon 10.

Here, we report on the second patient with a homozygous truncating *POCIA* mutation in exon 10, corroborating the view that *POCIA* mutations restricted to exon 10 are not associated with SOFT syndrome but cause a distinct condition characterized by extreme insulin resistance and short stature.

2. MATERIALS AND METHODS

2.1 Case description

The proband was a 42-year old woman of Southern Italy origin, born from first cousins. The father was healthy, while the mother presented osteoporosis and presenile Parkinson's disease with onset of the disease at 56 years of age.

Patient's first sign of disease was the appearance of acanthosis nigricans in the neck region at 7-8 years of age, initially noted by proband's mother. She had a premature menarche at 9 years old, followed by a worsening of acanthosis nigricans spreading to flexural areas including nasolabial folds, perioral region, armpits, perineum and ankles (Fig. 1A, B). She has short stature (138 cm, -4 SD), and normal intelligence. From childhood, she presented hands with dorsal swelling of the soft tissues (Fig. 1C). Until adolescence, foot also showed a dorsal bulge, dramatically reduced from 16-18 years of age. She also showed facial dysmorphism with micrognathia, prominent nose, low set ears, facial hirsutism that had been treated with laser therapy, alopecia and thinning hair (Fig. 1D) and eyebrows, in absence of nail and bone hypoplasia.

On clinical examination, she presented lumbar lordosis not associated either to skeletal dysplasia or "dog-like" vertebral bodies at radiological investigations (Fig. 1E). Contrariwise, a dysplastic pelvis was observed (Fig. 1E). At 41 years of age, a further radiological examination documented a mild knee arthrosis and bilateral patella osteosclerosis (Fig. 1F). Lastly, lumbosacral MRI did not show any transitional vertebrae (Fig. 1G).

At 14 years old, she was diagnosed with diabetes. She had severe fasting hyperinsulinemia, with high plasma levels of insulin after oral glucose tolerance test (120 min insulin level: 570 $\mu\text{U}/\mu\text{l}$, 180 min insulin level: 249 $\mu\text{U}/\mu\text{l}$). Her body mass index was within normal range (24.1 kg/m^2). Fasting glucose was normal until she reached 20 years of age. Thence, due to the persisting extreme insulin resistance, a combined therapy with metformin (1,500 mg/die) and insulin was introduced. At present, she is treated with fast-acting insulin (aspart 45 UI, three times/die) and long acting insulin (detemir 15 UI at night). In addition, she presented dyslipidemia with severe hypertriglyceridemia (350 mg/dl), mild hypercholesterolemia (220 mg/dl), and mild hyperuricemia. At recent examination, BMI remained within normal range but she showed a mild centripetal fat distribution and a fatty liver at abdominal ultrasonography.

She has a long history of irregular menstrual cycles since adolescence and an estroprogestinic therapy was introduced. At 40 years of age, she developed amenorrhea, which was associated with a hyperprolactinemia (PRL: 999 ng/ml) of unknown origin, with a further increasing 6 months later (PRL: 3,379 ng/ml). Total testosterone, LH, FSH and TSH were in normal range. Brain MRI did not reveal any pituitary lesion (Fig.1H). At 41 years, she was diagnosed with a bilateral carpal tunnel syndrome, and mild sensory motor symmetrical polyneuropathy at lower limbs likely due to diabetes.

2.2 Genetic studies

The proband and her mother provided written informed consent for the molecular analyses, and the study was approved by the internal Ethics Committee of the Department of Medical Sciences, University of Torino, Italy. Whole Exome Sequencing (WES) on the proband was outsourced to BGI-Shenzen using genomic DNA extracted from circulating leukocytes. Targeted enrichment was performed using SureSelect All Exon v4 kit (Agilent), and captured libraries were loaded onto an Illumina HiSeq 2000 platform (Illumina). WES data analysis was performed using an in-house

implemented pipeline⁸⁻¹⁰. High-quality variants were filtered by discarding those with MAF > 0.5% in ExAC 0.3 and with frequency > 2% in our in-house database. SnpEff toolbox v4.2¹¹ was used to predict the functional impact of variants, and retain missense/nonsense/frameshift changes, coding indels, and intronic variants at exon-intron junctions (within position -/+8). Functional annotation of variants was performed using snpEff v4.2 and dbNSFP2.9^{11,12}.

Based on consanguinity, we assumed an autosomal recessive model of inheritance for the trait, and retained all the homozygous variants located within LoH genomic stretches using Homozygosity Mapper¹³ (<http://www.homozygositymapper.org>), setting 80 as the number of consecutive homozygous SNPs. Variants were then filtered according to their predicted functional impact, retaining those variants with CADD score >15^{12,14}, and then prioritized taking into account the biological and clinical relevance of individual genes.

Sequence validation and segregation analyses were performed by Sanger sequencing using an ABI 3130XL and the ABI BigDye Terminator Sequencing Kit V 3.1 (Life Technologies). Sequences were examined using the SeqScape v2.6 Software (Life Technologies).

2.3 Gene expression studies

Patient's RNA was isolated from PAXgene-stabilized blood sample using the PAXgene blood RNA kit (PreAnalytix). Commercial RNAs extracted from cell lines representing ten different human tissues (Human MTC Panel I, #636742 and Human Fetal MTC Panel, #636747, Clontech Laboratories) were used to test tissue-specific expression of the two major *POCIA* isoforms. cDNA was generated using the MLV Transcriptase (Applied Biosystem, Wilmington, DE, USA) from 1µg of total RNA. To confirm the presence of both 10+ and 10- *POCIA* isoforms, patient's cDNA was amplified using primers already described in Chen et al., 2015 and PCR product was run on a 2% agarose gel stained with ethidium bromide. Bands were gel-purified and Sanger sequenced to confirm the presence of exon 9-exon10 and exon 9-exon11 junctions. *POCIA* expression was tested

with primers described in Chen et al., 2015. Amplified cDNAs were run on a 2% agarose gel and stained with Ethidium bromide. Bands intensities from tissues' cDNA were assessed using the ImageLAB software (Bio-Rad, Hercules, CA, USA). β -actin was used as reference to determine *POCIA* expression levels. The ratio between mRNA isoforms containing (10+) and lacking (10-) exon 10 was also evaluated.

3. RESULTS

3.1 Genetic Analysis and gene expression studies

WES statistics are reported in Supplementary Table 1. Data annotation predicted 13,841 high-quality variants having functional impact (*i.e.*, non-synonymous and splice site changes). Among them, 400 variants passed the public and in-house database filters and were taken into account for further analyses. Variants were then filtered to retain homozygous sequence changes located within LoH regions (Supplementary Table 2) with disruptive impact on protein structure/function predicted with confidence. Prioritization of the retained variants taking into account the biological relevance of individual genes allowed identifying *POCIA* as the best candidate disease gene. The proband carried a homozygous frameshift variant (c.1047_1048dupC, p.G337Rfs*25, NM_015426) affecting exon 10 of the gene. As expected, genotyping of maternal DNA confirmed the occurrence of the truncating variant at the heterozygous state, according to the recessive pattern of inheritance (Fig. 2 A, B).

POCIA gene had previously been reported to cause SOFT syndrome, whose clinical phenotype significantly differs from that of the present patient (Tab. 1). Of note, a single case with a homozygous *POCIA* mutation and clinical features overlapping those exhibited by the present patient has recently been reported⁷(Tab.1). Remarkably, this patient also carried a frameshift

mutation in exon 10 of the gene, differing from location of the previously reported *POC1A* mutations underlying SOFT syndrome (Fig. 2B).

RNA analysis performed on proband's cDNA confirmed the presence of the 10+ and the 10- *POC1A* isoforms (Fig.2C). Expression analysis on adult and embryonic tissues showed that *POC1A* mRNA level varies considerably among tissues, and that the mRNA isoform lacking exon 10 is significantly represented in the *POC1A* mRNA pool, being from 34% (adult frontal cortex) to 8,6% (adult stomach) (Fig. 2C), supporting the hypothesis of a less severe clinical impact of mutations affecting this exon.

4. DISCUSSION

Pleiotropy is a common phenomenon in Mendelian diseases, and mutations affecting genes with pleiotropic effects can frequently cause distinct phenotypes. Different molecular mechanisms underlie this phenomenon¹⁵. The pathogenic variants can affect diverse functional domains of the protein (*e.g.*, PHD-like *vs.* helicase domains in *ATRX*), have mild or severe impact on protein function (missense *vs.* truncating mutations), or cause quantitatively distinct effects (loss of function *vs.* gain of function mutations). In a few but instructive cases reported in literature, different classes of mutations have been shown to specifically affect distinct isoform of the protein. One example is represented by mutations in *PLEC* gene¹⁶. Changes affecting exons common to all eight *PLEC* isoforms cause epidermolysis bullosa simplex (EBS), whereas mutations located in the alternative exon 1a, disrupt specifically the skin-specific isoform of the protein (P1a) and cause a less severe condition in which the disorder is limited to epidermis without extra cutaneous involvement. We describe the second patient with a homozygous mutation in the *POC1A* gene not associated with SOFT syndrome, and whose clinical features overlap those of a previous subject reported by Chen *et al.*, 2015. Our case confirms that mutations in *POC1A* gene cause two distinct conditions: SOFT syndrome⁶ and a variant phenotype (variant *POC1A*-related, v*POC1A*, syndrome) characterized by

extreme insulin resistance and short stature . The main clinical differences between the two “phenotypes” include an extreme dyslipidemia with insulin resistance and acanthosis nigricans, which represent a major feature in vPOC1A syndrome, but do not occur in SOFT syndrome. Facial dysmorphism is more severe and distinctive of patients with SOFT syndrome, and ectodermal dysplasia has not been observed in the two reported cases with the vPOC1A phenotype (Table 1). SOFT-associated mutations are nonsense^{3,6} or missense^{2,5} changes that affect all the three POC1A isoforms, causing a complete loss of function (Fig. 2). On the other hand, patients affected by the vPOC1A syndrome carry mutations restricted to exon 10 of the *POC1A* gene and affect only two of the three POC1A isoforms, maintaining functional the protein lacking exon 10 encoded region (in frame 48 a.a. deletion). The residual function of the protein likely explains the overlapping features of SOFT and vPOC1A syndromes, which are milder in the latter. Furthermore, the insulin resistant hyperinsulinemia, a distinctive phenotype of vPOC1A patients, may be due to the unbalance of the 10+/10- isoforms present only in those patients.

Notably, *POC1A* encodes a protein associated with centrioles during the cell cycle and crucial for both mitotic spindle and primary ciliary function. Other genetic defects affecting the centrosome cause extreme insulin resistance with severe dyslipidaemia, such as Alström syndrome¹⁷ and Microcephalic Osteodysplastic Primordial Dwarfism type II (MOPDII)¹⁸, supporting a connection between dysregulated function of some centriolar and pericentriolar proteins and defective peripheral response to insulin and adipose tissue maintenance and regeneration.

In conclusion, biallelic mutations in *POC1A* gene cause two clinically distinct conditions: SOFT syndrome, which is characterized by short stature, onychodysplasia, facial dysmorphism, and hypotrichosis, and a less severe phenotype, vPOC1A, which major features include extreme insulin resistance and short stature and is specifically caused by mutations affecting exon 10 of the gene. The present findings point to this specific class of mutations in *POC1A* as the cause of cases with idiopathic insulin resistance and short stature.

5. DECLARATION OF INTEREST

We declare that there is no conflict of interest that could be perceived as prejudicing the impartiality of the research reported.

6. FUNDING

This work was supported in part by MURST60%, Associazione “E.E. Rulfo” (to A.B.), and Fondazione Bambino Gesù (to M.T.).

7. ACKNOWLEDGMENTS

We are grateful to the participating family.

8. REFERENCES

1. Venoux M, Tait X, Hames RS, Straatman KR, Woodland HR & Fry AM. Poc1A and Poc1B act together in human cells to ensure centriole integrity. *J Cell Sci* 2013 **126** 163-175.
2. Sarig O, Nahum S, Rapaport D, Ishida-Yamamoto A, Fuchs-Telem D, Qiaoli L, Cohen-Katsenelson K, Spiegel R, Nousbeck J, Israeli S, Borochowitz ZU, Padalon-Brauch G, Uitto J, Horowitz M, Shalev S & Sprecher E. Short stature, onychodysplasia, facial dysmorphism, and hypotrichosis syndrome is caused by a POC1A mutation. *Am J Hum Genet* 2012 **91** 337-342.
3. Barraza-Garcia J, Ivan Rivera-Pedroza C, Salamanca L, Belinchon A, Lopez-Gonzalez V, Sentchordi-Montane L, del Pozo A, Santos-Simarro F, Campos-Barros A, Lapunzina P, Guillen-Navarro E, Gonzalez-Casado I, Garcia-Minaur S & Heath KE. Two novel POC1A mutations in the primordial dwarfism, SOFT syndrome: Clinical homogeneity but also unreported malformations. *Am J Med Genet A* 2016 **170A** 210-216.
4. Ko JM, Jung S, Seo J, Shin CH, Cheong HI, Choi M, Kim OH & Cho TJ. SOFT syndrome caused by compound heterozygous mutations of POC1A and its skeletal manifestation. *J Hum Genet* 2016 **61** 561-564.
5. Koparir A, Karatas OF, Yuceturk B, Yuksel B, Bayrak AO, Gerdan OF, Sagioglu MS, Gezdirici A, Kirmintay K, Selcuk E, Karabay A, Creighton CJ, Yuksel A & Ozen M. Novel POC1A mutation in primordial dwarfism reveals new insights for centriole biogenesis. *Hum Mol Genet* 2015 **24** 5378-5387.
6. Shaheen R, Faqeh E, Shamseldin HE, Noche RR, Sunker A, Alshammari MJ, Al-Sheddi T, Adly N, Al-Dosari MS, Megason SG, Al-Husain M, Al-Mohanna F & Alkuraya FS. POC1A truncation mutation causes a ciliopathy in humans characterized by primordial dwarfism. *Am J Hum Genet* 2012 **91** 330-336.
7. Chen JH, Segni M, Payne F, Huang-Doran I, Sleigh A, Adams C, Consortium UK, Savage DB, O'Rahilly S, Semple RK & Barroso I. Truncation of POC1A associated with short stature and extreme insulin resistance. *J Mol Endocrinol* 2015 **55** 147-158.
8. Cordeddu V, Redeker B, Stellacci E, Jongejan A, Fragale A, Bradley TE, Anselmi M, Ciolfi A, Cecchetti S, Muto V, Bernardini L, Azage M, Carvalho DR, Espay AJ, Male A, Molin AM, Posmyk R, Battisti C, Casertano A, Melis D, van Kampen A, Baas F, Mannens MM, Bocchinfuso G, Stella L, Tartaglia M & Hennekam RC. Mutations in ZBTB20 cause Primrose syndrome. *Nat Genet* 2014 **46** 815-817.
9. Kortum F, Caputo V, Bauer CK, Stella L, Ciolfi A, Alawi M, Bocchinfuso G, Flex E, Paolacci S, Dentici ML, Grammatico P, Korenke GC, Leuzzi V, Mowat D, Nair LD, Nguyen TT, Thierry P, White SM, Dallapiccola B, Pizzuti A, Campeau PM, Tartaglia M & Kutsche K. Mutations in KCNH1 and ATP6V1B2 cause Zimmermann-Laband syndrome. *Nat Genet* 2015 **47** 661-667.
10. Niceta M, Stellacci E, Gripp KW, Zampino G, Kousi M, Anselmi M, Traversa A, Ciolfi A, Stabley D, Bruxelles A, Caputo V, Cecchetti S, Prudente S, Fiorenza MT, Boitani C, Philip N, Niyazov D, Leoni C, Nakane T, Keppler-Noreuil K, Braddock SR, Gillessen-Kaesbach G, Palleschi A, Campeau PM, Lee BH, Pouponnot C, Stella L, Bocchinfuso G, Katsanis N, Sol-Church K & Tartaglia M. Mutations Impairing GSK3-Mediated MAF Phosphorylation Cause Cataract, Deafness, Intellectual Disability, Seizures, and a Down Syndrome-like Facies. *Am J Hum Genet* 2015 **96** 816-825.
11. Cingolani P, Platts A, Wang le L, Coon M, Nguyen T, Wang L, Land SJ, Lu X & Ruden DM. A program for annotating and predicting the effects of single nucleotide polymorphisms, SnpEff: SNPs in the genome of *Drosophila melanogaster* strain w1118; iso-2; iso-3. *Fly (Austin)* 2012 **6** 80-92.
12. Liu X, Jian X & Boerwinkle E. dbNSFP v2.0: a database of human non-synonymous SNVs and their functional predictions and annotations. *Hum Mutat* 2013 **34** E2393-2402.
13. Seelow D & Schuelke M. HomozygosityMapper2012--bridging the gap between homozygosity mapping and deep sequencing. *Nucleic Acids Res* 2012 **40** W516-520.
14. Kircher M, Witten DM, Jain P, O'Roak BJ, Cooper GM & Shendure J. A general framework for estimating the relative pathogenicity of human genetic variants. *Nat Genet* 2014 **46** 310-315.
15. Zhu X, Need AC, Petrovski S & Goldstein DB. One gene, many neuropsychiatric disorders: lessons from Mendelian diseases. *Nat Neurosci* 2014 **17** 773-781.

16. Gostynska KB, Nijenhuis M, Lemmink H, Pas HH, Pasmooij AM, Lang KK, Castanon MJ, Wiche G & Jonkman MF. Mutation in exon 1a of PLEC, leading to disruption of plectin isoform 1a, causes autosomal-recessive skin-only epidermolysis bullosa simplex. *Hum Mol Genet* 2015 **24** 3155-3162.
17. Collin GB, Marshall JD, Ikeda A, So WV, Russell-Eggitt I, Maffei P, Beck S, Boerkoel CF, Sicolo N, Martin M, Nishina PM & Naggert JK. Mutations in ALMS1 cause obesity, type 2 diabetes and neurosensory degeneration in Alstrom syndrome. *Nat Genet* 2002 **31** 74-78.
18. Willems M, Genevieve D, Borck G, Baumann C, Baujat G, Bieth E, Edery P, Farra C, Gerard M, Heron D, Leheup B, Le Merrer M, Lyonnet S, Martin-Coignard D, Mathieu M, Thauvin-Robinet C, Verloes A, Colleaux L, Munnich A & Cormier-Daire V. Molecular analysis of pericentrin gene (PCNT) in a series of 24 Seckel/microcephalic osteodysplastic primordial dwarfism type II (MOPD II) families. *J Med Genet* 2010 **47** 797-802.

9. FIGURE LEGENDS.

Figure 1. Clinical and neuroradiological findings.

A) Acanthosis nigricans in nasolabial folds and perioral region. B) Acanthosis nigricans of the flexural area of the ankle; right foot with dorsal swelling of the soft tissues. Shortening of the fourth metatarsal. C) Dorsal hand swelling of the soft tissues. D) Alopecia and thinning hair. E-G) X-ray images showing the hypoplastic pelvis (E). In panel F, mild bilateral knee osteoarthritis. Lumbosacral MRI (G) excluded any transitional vertebrae described in the other patient with *POCIA* pathogenic variant in exon 10⁷. H) Cranial MRI did not reveal any pituitary lesion.

Figure 2: Molecular findings.

A) Pedigree of the family reporting the segregation of the pathogenic variant. Black symbol and arrow indicate the affected case (proband). A line above symbols indicates DNA availability. The sequence chromatogram showing the disease-causing mutation, c.1007_1008dupC (p.Gly337Argfs*25) in the *POCIA* gene, is reported. B) Structure of the three cDNA isoforms and predicted protein of *POCIA* are illustrated. On the left the corresponding accession numbers. Exons of the *POCIA* gene are distinct into coding (colored boxes) and non-coding (small black boxes). The corresponding functional domains are shown at protein level [N-terminal seven-bladed β -propeller WD40 domain (green); C-terminal coiled-coil domain that includes the highly conserved

Poc1 motif (light blue)]. All reported pathogenic variant are in homozygous state with the exception of a patient compound heterozygous (underlined). In black, pathogenic changes associated with SOFT syndrome; in red, pathogenic changes associated with IRSS syndrome. The c.1007_1008dupC (p.Gly337Argfs*25) variant identified in our patient is boxed. C) *POC1A* cDNA analysis. On the upper part, gel electrophoresis of patient's cDNA showing 10+ and 10- *POC1A* isoforms. The splicing junctions (exon9-exon10 and exon9-exon11) were Sanger sequenced. On the lower part, *POC1A* expression analysis. Histograms indicate tissue-specific expression of total *POC1A* (in yellow) and the ratio between mRNA isoforms containing (exon 10+) or lacking (exon 10-) exon 10 (in light blue). From left to right, tissue analyzed were human adult brain, adult cerebellum, adult frontal cortex, fetal brain, adult heart, adult kidney, adult lung, adult placenta, adult stomach, and adult blood.

Supplementary Materials

Supplementary Table 1. WES characteristics and data output.

| | |
|--|--|
| WES enrichment kit | SureSelect Human All Exon V4 (Agilent) |
| Sequencing platform | Illumina HiSeq 2000 |
| N° reads | 72,232,178 |
| Mean read length | 100 |
| Duplication rate | 11 |
| Target regions coverage | 97.9 |
| Target regions coverage > 20x | 80.6 |
| Average depth on target | 58x |
| Total number of variants | 55,382 |
| Variants with effect on CDS or affecting splice sites ¹ | 13,841 |
| Variants with low or unknown frequency ² | 400 |
| Homozygous variants | 32 |
| | |
| ¹ High-quality nonsynonymous single nucleotide variants and indels within coding sequence and intronic stretches flanking splice sites (-/+8) ² ExAC v.0.3 with low (<0.1%) or unknown MAF and with frequency <2% in our in-house database (approx. 700 population-matched exomes). | |

Supplementary Table 2. List of the identified homozygous variants by WES analysis.

| gene Name | Effect | AA substitution | CADD phred score |
|-----------------|--|--------------------|------------------|
| <i>ABCC5</i> | missense | p.Lys733Arg | 15.26 |
| <i>ALDH1L2</i> | missense | p.Thr87Ala | 3.278 |
| <i>ATXN2</i> | disruptive_inframe_deletion | p.Gln180_Gln187del | 10.11 |
| <i>BCL6</i> | missense | p.Gln397His | 21.9 |
| <i>CAMKK2</i> | frameshift | p.Gly539fs | 9.062 |
| <i>CNTNAP3B</i> | splice_region | . | 3.224 |
| <i>COL22A1</i> | splice_donor | . | 24.3 |
| <i>CYLD</i> | 5_prime_UTR_premature_start_codon_gain | . | 6.778 |
| <i>DDX54</i> | missense | p.Ala512Thr | 17.9 |
| <i>DNAH7</i> | splice_region | . | 5.982 |

| | | | |
|---------------------|--|-------------------------|-------|
| <i>GOLGA80</i> | missense | p.Asn33Lys | 0.001 |
| <i>HEATR5A</i> | missense | p.Cys1951Tyr | 25 |
| <i>HLA-DQB1</i> | missense | p.Ser229Asn | 18.99 |
| <i>ITPR3</i> | missense | p.Ser272Phe | 26.7 |
| <i>KEL</i> | missense | p.Arg728Cys | 29 |
| <i>KRTAP5-5</i> | frameshift | p.Ala53fs | 22 |
| <i>KTN1</i> | frameshift | p.Gln961fs | 27.8 |
| <i>LOC100287944</i> | splice_region | . | 15.94 |
| <i>MBD3L5</i> | missense | p.Arg51Thr | 18.9 |
| <i>P2RX7</i> | missense | p.Arg276Cys | 35 |
| <i>PELI2</i> | missense | p.Arg325Gln | 25.4 |
| <i>POCIA</i> | frameshift | p.Gly337Argfs*25 | 32 |
| <i>REST</i> | missense | p.Glu115Gly | 23.5 |
| <i>RNF123</i> | splice_region | . | 5.401 |
| <i>RRAS</i> | missense | p.Ala157Gly | 15.55 |
| <i>SAC3D1</i> | missense | p.Val108Met | 26.1 |
| <i>SPATA31A5</i> | missense | p.His301Pro | 13.24 |
| <i>TTC14</i> | missense | p.Leu75Val | 25.6 |
| <i>ZNF106</i> | 5_prime_UTR_premature_start_codon_gain | . | 0.066 |
| <i>ZNF148</i> | splice_region | . | 11.62 |
| <i>ZNF662</i> | missense | p.Arg347Gln | 10.17 |
| <i>ZNF860</i> | missense | p.Cys543Arg | 23.1 |

The predicted functional impact of high-quality private, rare and clinically associated homozygous variants was assessed by CADD tool. Low priority variants (CADD score < 15) are reported with gray background.

Figure 1

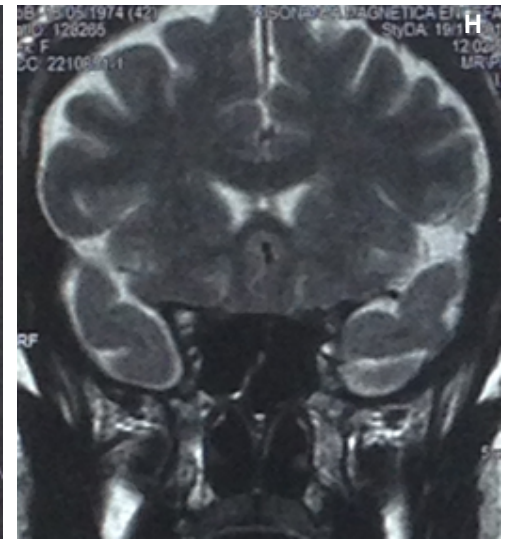
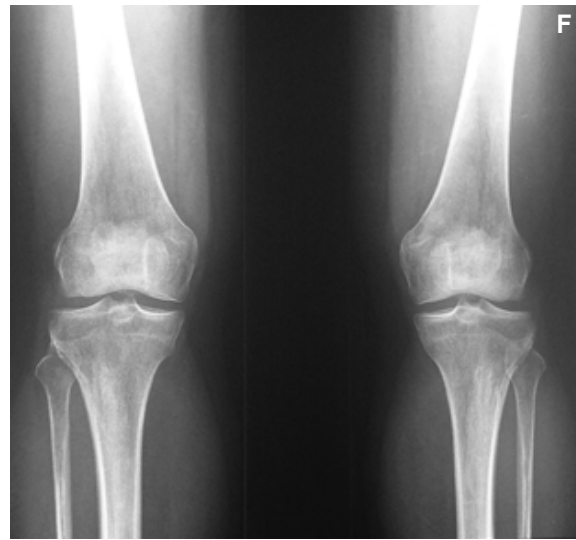
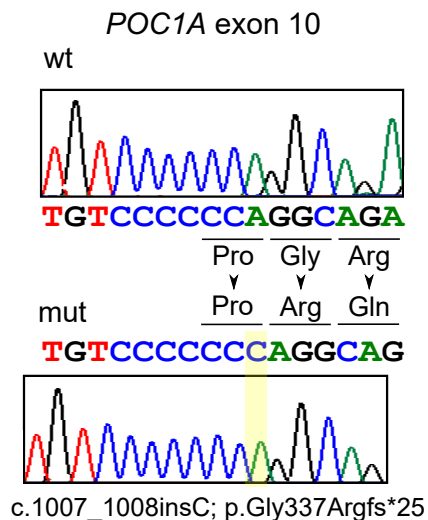
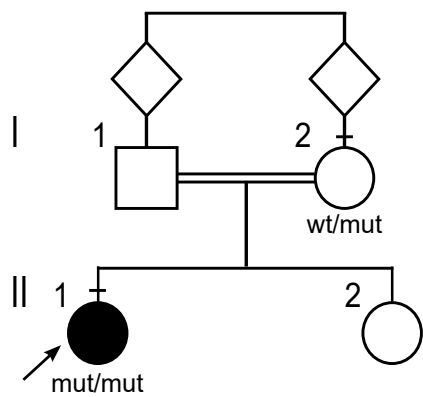
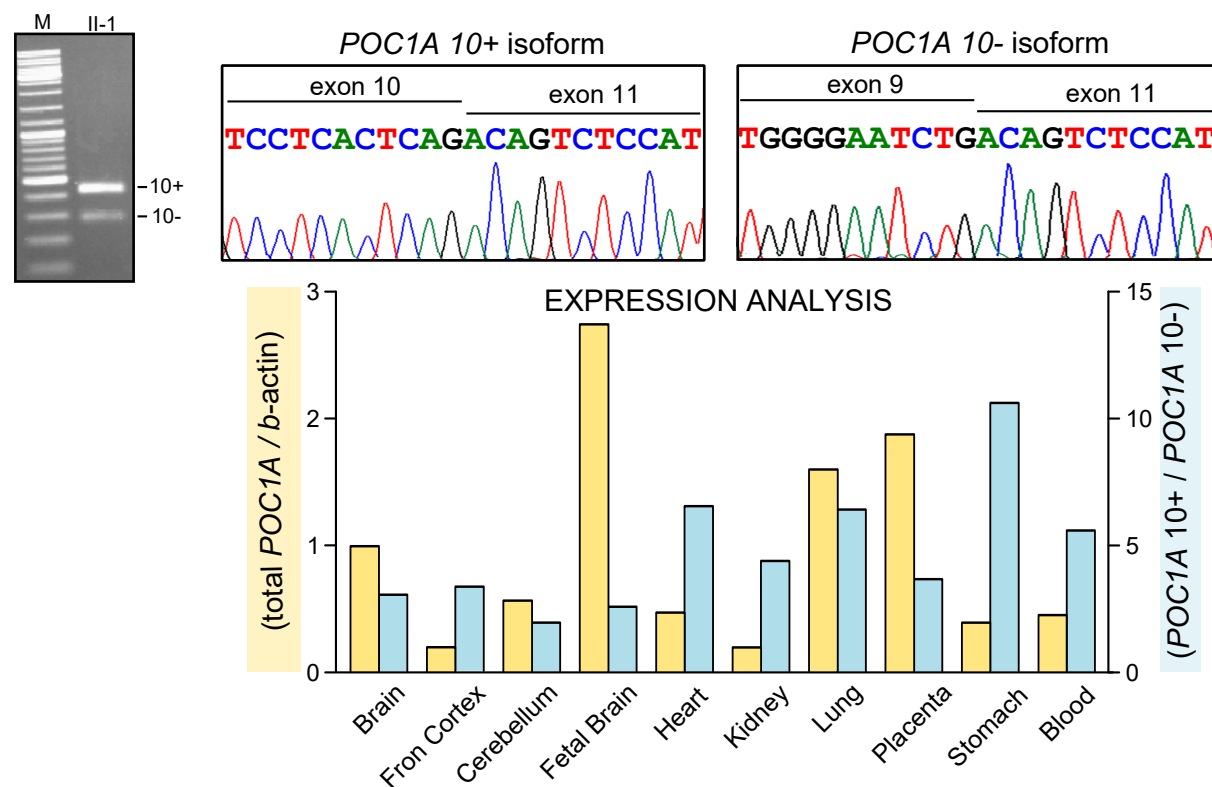


Figure 2

A)



C)



B)

